IJMPR, 2026, 10(4), 20-32 **ISSN: 2319-5878**

INTERNATIONAL JOURNAL OF MODERN PHARMACEUTICAL RESEARCH

www.ijmpronline.com

Research Article

Impact Factor: 7.533

Coden USA: IJMPR3

IN SILICO DEVELOPMENT OF A QSAR MODEL FOR ANTI VIRAL COMPOUNDS

Aruna Rajubabu*, D. Krishna Teja[2], Dr. V. Padmaja[3], Prof. M. Sumakanth[4]

[1,2,3,4]Department of Pharmaceutical Chemistry, RBVRR Women's College of Pharmacy, Barkatpura, Hyderabad, Telangana.

Article Received on: 28/02/2026 **Article Revised on: 19/03/2026** **Article Published on: 01/04/2026**

***Corresponding Author**

Aruna Rajubabu

Department of Pharmaceutical Chemistry, RBVRR Women's College of Pharmacy, Barkatpura, Hyderabad, Telangana.

https://doi.org/10.5281/zenodo.19337139

How to cite this Article: Aruna Rajubabu*, D. Krishna Teja[2], Dr. V. Padmaja[3], Prof. M. Sumakanth[4] (2026). In Silico Development Of A Qsar Model For Anti Viral Compounds. International Journal of Modern Pharmaceutical Research, 10(4), 20–32.

ABSTRACT

Owing to the rising resistance and side effects associated with current antiviral therapies, there is a pressing need for the development of novel antiviral agents with improved efficacy and safety profiles. In this study, an in silico QSAR (Quantitative Structure–Activity Relationship) model was developed to predict the antiviral activity of chemically diverse compounds. A dataset of molecules with reported Anti-HIV activity was retrived from Pubchem, and their IC_{50} values were converted to PIC_{50}. The compounds included a wide range of heterocyclic scaffolds known for HIV Integrase inhibitors properties. Molecular descriptors calculation was performed using ChemMaster (1.2 Basic free) software. The QSAR model was built using regression based method to identify key molecular features contributing to Antiviral potency. The model was validated, demonstrating strong predictive reliability. This computational approach offers valuable insights into structure–activity relationships and facilitates the novel Anti- HIV agents with enhanced therapeutic potential.

KEYWORDS: HIV Integrase inhibitors, QSAR modeling, ChemMaster(1.2 Basic free) software, Molecular descriptors.

INTRODUCTION

HIV- Human Immunodeficiency Virus is the causative agent of Acquired Immunodeficiency Syndrome (AIDS). HIV weakens the immune system by infecting and destroying CD4+ T cells, which are vital for protecting the body against infections. The virus Is in maximum instances transmitted via unprotected sexual contact, sharing of inflamed needles, and from mother to little one at some stage in childbirth or breastfeeding. Once inside the body, HIV rapidly spreads through mucosal tissues and lymphoid organs, establishing a chronic infection. Early diagnosis and consistent use of Antiretroviral therapy (ART), the virus can be effectively suppressed, allowing individuals to maintain a strong immune system and lead long, healthy lives.[1]

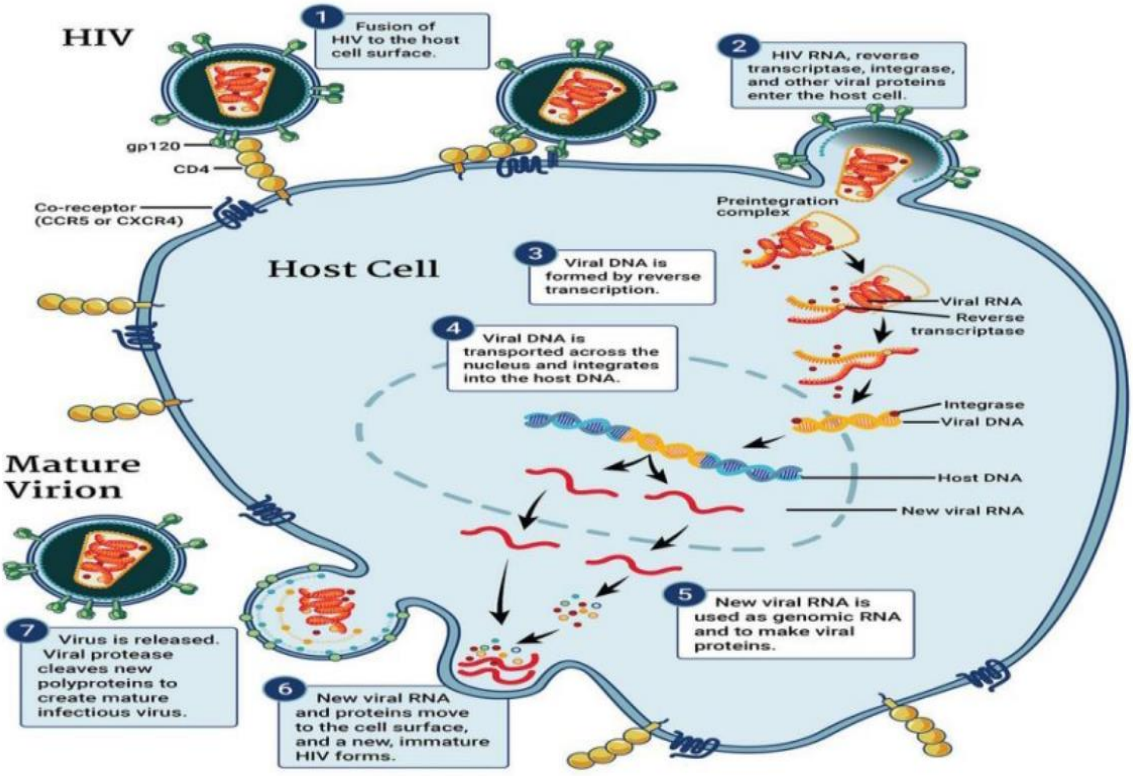

Figure 1: HIV replication cycle.[2]

CLASSIFICATION OF ANTI RETROVIRAL DRUGS

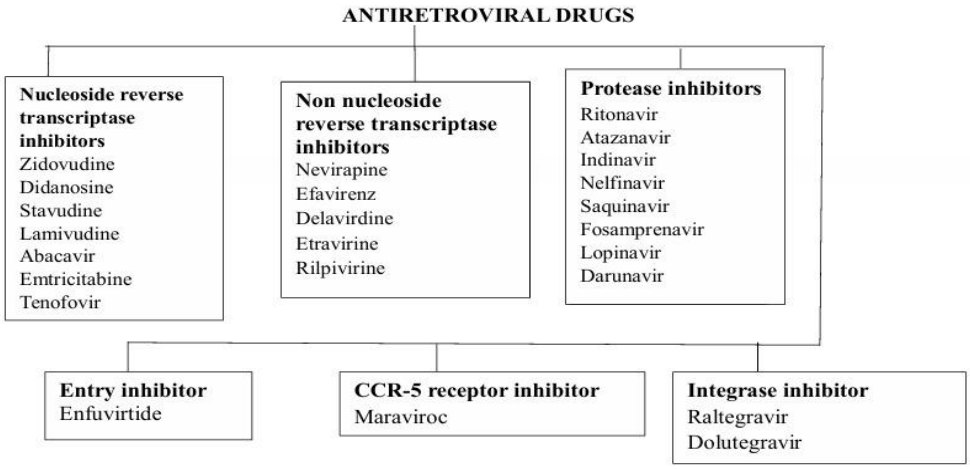

Figure 2: Anti Retroviral drugs.[3]

MOA OF ANTI RETROVIRAL DRUGS

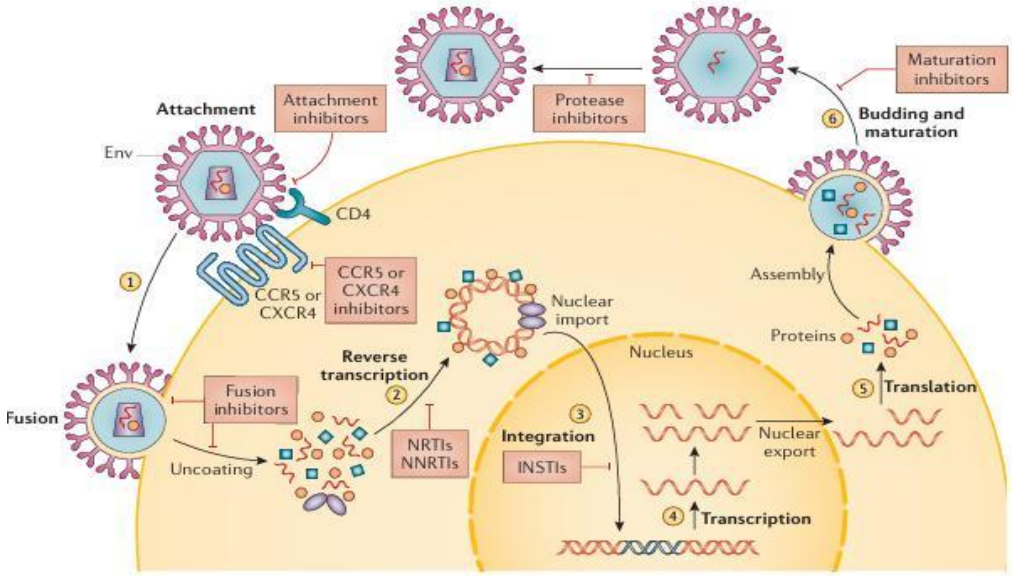

Figure 3: Sites of Antiretroviral Drug Action.[4]

HIV INTEGRASE

HIV Integrase is an Enzyme produced by a retrovirus (an RNA virus, such as HIV-1, which replicates in a host cell) that allows the viral DNA cloth to be included into the DNA of the infected. It is also produced for the same purpose by viruses containing double-stranded DNA. Integration of viral DNA into the host DNA is a crucial step in the replication of HIV-1.[5]

Role of integrase in viral replication

Integrase catalyzes at the least three reactions.

i. 3′ processing, formation of the preintegrase complex, and strand transfer. Briefly, as soon as the viral RNA is retrotranscribed into DNA through opposite transcriptase, integrase eliminates a 3’ terminal portion. At each ends of the newly shaped DNA in which it stays bound, stabilizing the preintegrase complex.

ii. Once 3’ processing occurs, the preintegrase complex (PIC) can shape which includes ring-formed viral DNA with related virus and host proteins. This complicated shape is capable of translocate throughout the nuclear membrane and into the nucleus.

iii. The very last response catalyzed via way of means of integrase is the strand switch wherein each 3’ ends of the DNA are Inserted into the host DNA or chromosome. The newly altered host DNA, which now consists of the HIV DNA, calls for restore that's executed with mobile DNA restore enzymes. . If strand switch in inhibited, the viral ring systems continue to be withinside the nuclear cytoplasm, the scientific relevance of that's unknown.

These reactions are Mg^{2+}-based in physiological conditions. Inhibitors of integrase which have now been evolved are strand transfer inhibitors (INSTIs) that block the insertion position on the host DNA.[6]

APPROVED INTEGRASE INHIBITORS

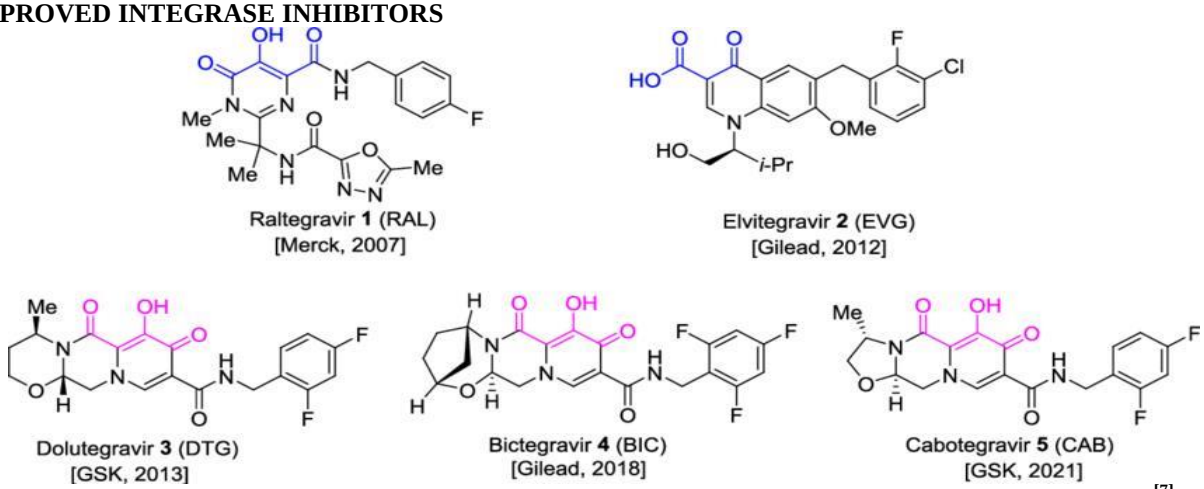

Figure 4: Chemical structures of FDA-approved INSTIs with company and year of FDA approval.[7]

QSAR (QUANTITATIVE STRUCTURE-ACTIVITY RELATIONSHIP)

Quantitative structure-interest relationship (QSAR) technique is based at the primary precept of chemistry that states that the organic interest (biological activity) of any ligand or compound is associated with the arrangement of atoms forming the molecular structure. This structural information can be defined in terms of a series of parameters called molecular descriptors. The biological activity is represented as a function of these molecular descriptors as depicted in equation.

Biological response or activity = *f* (molecular descriptor).[8]

TYPES OF QSAR

QSAR methodologies can be classified based on several criteria.

- **Based on Descriptor Dimensionality**

✓ 1D-QSAR correlating interest with international molecular residences like pKa, log P etc.
✓ 2D-QSAR correlating interest with structural styles like connectivity indices, 2D-Pharmacophores etc., with out taking into consideration the 3D-illustration of these properties.
✓ 3D-QSAR correlating activity with non-covalent interaction fields surrounding the molecules (e.g., CoMFA, CoMSIA).
✓ 4D-QSAR moreover which includes ensemble of ligand configurations in 3D-QSAR
✓ 5D-QSAR explicitly representing different induced-fit models in 4D-QSAR
✓ 6D-QSAR further incorporating different solvation models in 5D-QSAR.[9]

- **By Predicted Activity/Property**

✓ QSTR: Quantitative Structure-toxicity Relationship.
✓ QSMR: Quantitative Structure-metabolism Relationship.
✓ QSRR: Quantitative Structure-reactivity/retention Relationship.
✓ QSPR: Quantitative Structure-property (physicochemical) Relationship.

- **By Analysis Type**

✓ **Linear:** Linear statistical models like linear regression and partial regression,
✓ **Non-linear:** Non-linear/machine learning models Ex: artificial neural networks.

- **By Binding Nature**

✓ Receptor-dependent: Uses receptor structure.
✓ Receptor-independent: Ligand only.

STEPS INVOLVED IN QSAR MODEL GENERATION

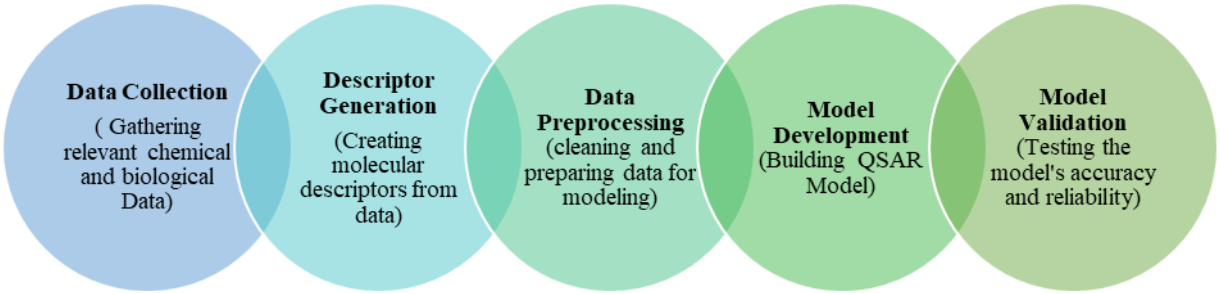

Software for QSAR Studies and Modeling are ADMET Predictor, OECD QSAR Application
Toolbox, PASS, TerraQSAR, VEGA-QSAR, WEBCDK, VCCL.[8]

HQSAR (Hologram Quantitative Structural Activity Relationship)

Hologram Quantitative Structure–Activity Relationship (HQSAR) is a 2D-QSAR technique that correlates biological activity with structural fragments by converting a compound's chemical representation into a molecular hologram. This approach eliminates the need for 3D structures, molecular alignment, and conformation specification.

- The HQSAR modeling analyses, calculations and visualizations have been done the usage of the SYBYL-X 1.zero package (Tripos Inc., St. Louis, MO, USA).
- The generation of the molecular fragments was carried out using several combinations of the following fragment distinction parameters: atoms (A), bonds (B), connections (C), hydrogen atoms (H), chirality (CH), and donor & acceptor (DA).
- Several combos of those parameters had been taken into consideration the usage of fragment length of default 4–7. Each unique fragment in the data set is assigned a large positive integer by means of a cyclic redundancy check (CRC) algorithm.
- Each integer corresponds to a bin in an integer array of constant period L (normally inside 12 default Hologram lengths of 53, 59, 61, 71, 83, 97, 151, 199, 257, 307, 353, and 401 bins). Thus, All generated fragments are hashed into array boxes withinside the variety of one to L. This array now Constitutes a molecular hologram, the bin occupancies being the descriptor values. The

following wellknown PLS evaluation identifies a set of explanatory variables.[10,11]

PUBCHEM

PubChem (http://pubchem.ncbi.nlm.nih.gov) is a public repository for chemical structures and their biological properties. The bioactivity results in PubChem are contributed by more than a hundred organizations, with the majority of data coming from the screening center network under the NIH Molecular Libraries Program (MLP).[12]

Users accessed PubChem for various types of data, with the most frequent being.

1. **Chemical Structures:** Downloaded in formats such as **SMILES**, **InChI**, and **SDF,** Structural images accessed via the web interface.

2. Basic Small Molecule Information: Annotations, synonyms, MeSH terms, Chemical formula and physicochemical properties (e.g., log P, molecular weight, number of hydrogen bond donors/acceptors) and Pharmacological data

3. PubChem Fingerprints: used for similarity searches**,** chemical space analysis**,** structure clustering**,** and SAR (Structure-Activity Relationship) studies.

4. Bioassay Datasets: Includes high-throughput screening (HTS) biochemical and cell- based assays, Utilized for SAR studies and data mining.

5. The PubChem identifiers (i.e. CID for Compound file, SID for Substance file and AID for BioAssay file) have been normally followed as a method for records and statistics change amongst diverse research and have been listed or recognized by various databases or tools.[13]

CHEMMASTER

ChemMaster is a versatile and comprehensive QSAR modeling & cheminformatics software that includes complete set of features for QSAR modeling and general cheminformatics & drug design tasks. The main features include.

- QSAR): Complete QSAR modeling functions including: Structure preparation, Descriptors & fingerprints calculation, Dataset division, Model improvement with various strategies together with more than one linear regression (MLR), aid vector regression (SVR) and k-Nearest Neighbors (kNN), Model validation & reporting.
- **Various QSAR Methods:** Regression (numerical) QSAR, Binary (classification) QSAR, Hologram-QSAR (HQSAR), Automatic-QSAR
- **Essential Cheminformatics & Drug Design Features:** Substructure search & records filtering, customizable chemical plotting functionalities, Descriptors & fingerprints computation.
- **Advanced Cheminformatics & Drug Design Features:** Conformers generation, Similarity compuation, Clustering, Principal component analysis (PCA), Correlation analysis and Maximum common substructure (MCS) Analysis.
- **Modern & Easy To Use User Interface.[14]**

EXPERIMENTAL METHODOLOGY

QSAR Analysis

Data Collection

To develop a QSAR model for substituted thiazole derivatives as HIV integrase inhibitors, relevant biological data were first collected from the PubChem database (https://pubchem.ncbi.nlm.nih.gov/). Using specific keywords such as "substituted thiazoles HIV integrase inhibitors", a search was conducted to identify appropriate BioAssay entries, particularly those with publicly available IC_{50} values. Among the retrieved assays, datasets containing a significant number of biologically active compounds with clearly reported IC_{50} values were selected by identifying the corresponding AID (Assay Identifier). Upon selecting a relevant BioAssay, the associated compound data were accessed via the Data Table section. The dataset of active compounds only was downloaded by clicking on the CSV save button under the “Data Table (Active)” section. This file, in Excel-readable format, contains structural information, assay details, and IC_{50} values of active molecules. The chemical names of the substituted thiazoles along with their observed pIC_{50} values were shown in Table 1.

Table 1: The chemical names of the substituted thiazoles along with their respective pIC50 values in µM.[15]

S.No	COMPOUND NAME	Integrase IC_{50} Value(µM)	Integrase PIC_{50} value(µM)
1	(4R)-4-(azetidine-1-carbonyl)-7-[5-[(4-fluorophenyl)methyl]-1,3,4-thiadiazol-2-yl]-4-methyl-9-phenylmethoxy-2-propan-2-yl-3H-pyrido[1,2-a]pyrazine-1,8-dione	0.013	7.8861
2	(3S)-7-[5-[(4-fluorophenyl)methyl]-1,3,4-thiadiazol-2-yl]-9-hydroxy-3-(methoxymethyl)-2-propan-2-yl-3,4-dihydropyrido[1,2-a]pyrazine-1,8-dione	0.0085	8.0706
3	(4S)-7-[5-[(4-fluorophenyl)methyl]-1,3,4-thiadiazol-2-yl]-9-hydroxy-4-methyl-2-propan-2-yl-3,4-dihydropyrido[1,2-a]pyrazine-1,8-dione	0.0074	8.1308
4	7-[5-[(2,4-difluorophenyl)methyl]-1,3-thiazol-2-yl]-4-[(1,3-dioxoisoindol-2-yl)methyl]-4-methyl-9-phenylmethoxy-2-propan-2-yl-3H-pyrido[1,2-a]pyrazine-1,8-dione	0.013	7.8861
5	(3S)-2-(cyclopropylmethyl)-7-[5-[(4-fluorophenyl)methyl]-1,3,4-thiadiazol-2-yl]-9-hydroxy-3-(methoxymethyl)-3,4-dihydropyrido[1,2-a]pyrazine-1,8-dione	0.0088	8.0555
6	7-[5-[(2,4-difluorophenyl)methyl]-1,3,4-thiadiazol-2-yl]-9-hydroxy-4-(methoxymethyl)-2-propan-2-yl-3,4-dihydropyrido[1,2-a]pyrazine-1,8-dione	0.0082	8.0862

7	7-[5-[(2,4-difluorophenyl)methyl]-1,3-thiazol-2-yl]-9-hydroxy-4-(hydroxymethyl)-2-propan-2-yl-3,4-dihydropyrido[1,2-a]pyrazine-1,8-dione	0.0081	8.0915
8	2-[7-[5-[(2,4-difluorophenyl)methyl]-1,3-thiazol-2-yl]-9-hydroxy-1,8-dioxo-2-propan-2-yl-3,4-dihydropyrido[1,2-a]pyrazin-4-yl]-N,N-dimethylacetamide	0.0094	8.0269
9	7-[5-[(2,4-difluorophenyl)methyl]-1,3-thiazol-2-yl]-9-hydroxy-N,4-dimethyl-1,8-dioxo-2-propan-2-yl-3H-pyrido[1,2-a]pyrazine-4-carboxamide	0.01	8
10	2-cyclopropyl-7-[5-[(2,4-difluorophenyl)methyl]-1,3,4-thiadiazol-2-yl]-9-hydroxyspiro[3H-pyrido[1,2-a]pyrazine-4,4'-oxane]-1,8-dione	0.009	8.0458
11	2-[7-[5-[(2,4-difluorophenyl)methyl]-1,3-thiazol-2-yl]-9-hydroxy-1,8-dioxo-2-propan-2-yl-3,4-dihydropyrido[1,2-a]pyrazin-4-yl]-N-propan-2-ylacetamide	0.013	7.8861
12	(4R)-7-[5-[(2,4-difluorophenyl)methyl]-1,3,4-thiadiazol-2-yl]-9-hydroxy-4-(2-methoxyethoxymethyl)-2-propan-2-yl-3,4-dihydropyrido[1,2-a]pyrazine-1,8-dione	0.0081	8.0915
13	(4R)-7-[5-[(2,4-difluorophenyl)methyl]-1,3,4-thiadiazol-2-yl]-9-hydroxy-4-(2-methoxyethoxymethyl)-2-(2-methylpropyl)-3,4-dihydropyrido[1,2-a]pyrazine-1,8-dione	0.011	7.9586
14	(4S)-7-[5-[(2,4-difluorophenyl)methyl]-1,3,4-thiadiazol-2-yl]-9-hydroxy-4-(2-methoxyethoxymethyl)-2-(2-methylpropyl)-3,4-dihydropyrido[1,2-a]pyrazine-1,8-dione	0.012	7.9208
15	7-[5-[(2,4-difluorophenyl)methyl]-1,3,4-thiadiazol-2-yl]-9-hydroxy-1,8-dioxo-2-propan-2-yl-3,4-dihydropyrido[1,2-a]pyrazine-3-carboxylic acid	0.0064	8.1938
16	7-[5-[(2,4-difluorophenyl)methyl]-1,3-thiazol-2-yl]-9-hydroxy-4-methyl-4-(morpholine-4-carbonyl)-2-propan-2-yl-3H-pyrido[1,2-a]pyrazine-1,8-dione	0.013	7.8861
17	(4R)-7-[5-[(2,4-difluorophenyl)methyl]-1,3-thiazol-2-yl]-9-hydroxy-4-(2-methoxyethoxymethyl)-2-propan-2-yl-3,4-dihydropyrido[1,2-a]pyrazine-1,8-dione	0.01	8
18	(4R)-7-[5-[(2,4-difluorophenyl)methyl]-1,3-thiazol-2-yl]-9-hydroxy-4-(2-methoxyethoxymethyl)-2-(2-methylpropyl)-3,4-dihydropyrido[1,2-a]pyrazine-1,8-dione	0.011	7.9586
19	7-[5-[(2,4-difluorophenyl)methyl]-1,3-thiazol-2-yl]-9-hydroxy-3-(methoxymethyl)-2-(2-methylpropyl)-3,4-dihydropyrido[1,2-a]pyrazine-1,8-dione	0.0092	8.0362
20	7-[5-[(2,4-difluorophenyl)methyl]-1,3,4-thiadiazol-2-yl]-9-hydroxy-4-(methoxymethyl)-2-(2-methylpropyl)-3,4-dihydropyrido[1,2-a]pyrazine-1,8-dione	0.0083	8.0809
21	7-[5-[(2,4-difluorophenyl)methyl]-1,3,4-thiadiazol-2-yl]-9-hydroxy-1,8-dioxo-2-propan-2-yl-3,4-dihydropyrido[1,2-a]pyrazine-3-carbonitrile	0.0061	8.2147
22	N-[[7-[5-[(2,4-difluorophenyl)methyl]-1,3-thiazol-2-yl]-9-hydroxy-1,8-dioxo-2-propan-2-yl-3,4-dihydropyrido[1,2-a]pyrazin-4-yl]methyl]propanamide	0.0098	8.0088
23	N-[[7-[5-[(2,4-difluorophenyl)methyl]-1,3-thiazol-2-yl]-9-hydroxy-1,8-dioxo-2-propan-2-yl-3,4-dihydropyrido[1,2-a]pyrazin-4-yl]methyl]-2-methylpropanamide	0.013	7.8861
24	7-[5-[(2,4-difluorophenyl)methyl]-1,3,4-thiadiazol-2-yl]-9-hydroxy-3,3-dimethyl-2-(oxolan-3-yl)-4H-pyrido[1,2-a]pyrazine-1,8-dione	0.0089	8.0506
25	N-cyclopropyl-2-[7-[5-[(2,4-difluorophenyl)methyl]-1,3-thiazol-2-yl]-9-hydroxy-1,8-dioxo-2-propan-2-yl-3,4-dihydropyrido[1,2-a]pyrazin-4-yl]acetamide	0.011	7.9586
26	2-[7-[5-[(2,4-difluorophenyl)methyl]-1,3,4-thiadiazol-2-yl]-9-hydroxy-1,8-dioxo-2-propan-2-yl-3,4-dihydropyrido[1,2-a]pyrazin-3-yl]-N,N-dimethylacetamide	0.0091	8.041
27	7-[5-[(2,4-difluorophenyl)methyl]-1,3-thiazol-2-yl]-9-hydroxy-1,8-dioxo-2-propan-2-yl-3,4-dihydropyrido[1,2-a]pyrazine-4-carbonitrile	0.0064	8.1938
28	N-[[7-[5-[(2,4-difluorophenyl)methyl]-1,3-thiazol-2-yl]-9-hydroxy-1,8-dioxo-2-propan-2-yl-3,4-dihydropyrido[1,2-a]pyrazin-4-yl]methyl]-N-methylacetamide	0.0098	8.0088
29	(3S)-2-cyclobutyl-7-[5-[(4-fluorophenyl)methyl]-1,3,4-thiadiazol-2-yl]-9-hydroxy-3-(2-methoxyethoxymethyl)-3,4-dihydropyrido[1,2-a]pyrazine-1,8-dione	0.011	7.9586
30	(4R)-7-[5-[(2,4-difluorophenyl)methyl]-1,3,4-thiadiazol-2-yl]-9-hydroxy-4-(methoxymethyl)-2-propan-2-yl-3,4-dihydropyrido[1,2-a]pyrazine-1,8-dione	0.0075	8.1249
31	(4R)-2-cyclobutyl-7-[5-[(2,4-difluorophenyl)methyl]-1,3,4-thiadiazol-2-yl]-9-hydroxy-4-(2-methoxyethoxymethyl)-3,4-dihydropyrido[1,2-a]pyrazine-1,8-dione	0.0095	8.0223
32	(4S)-7-[5-[(2,4-difluorophenyl)methyl]-1,3,4-thiadiazol-2-yl]-9-hydroxy-4-(methoxymethyl)-2-propan-2-yl-3,4-dihydropyrido[1,2-a]pyrazine-1,8-dione	0.0077	8.1135
33	(4S)-7-[5-[(4-fluorophenyl)methyl]-1,3,4-thiadiazol-2-yl]-9-hydroxy-4-(methoxymethyl)-2-propan-2-yl-3,4-dihydropyrido[1,2-a]pyrazine-1,8-dione	0.0087	8.0605
34	(4R)-2-cyclobutyl-7-[5-[(4-fluorophenyl)methyl]-1,3,4-thiadiazol-2-yl]-9-hydroxy-4-(methoxymethyl)-3,4-dihydropyrido[1,2-a]pyrazine-1,8-dione	0.0087	8.0605
35	(3S)-2-cyclobutyl-7-[5-[(2,4-difluorophenyl)methyl]-1,3,4-thiadiazol-2-yl]-9-hydroxy-3-(methoxymethyl)-3,4-dihydropyrido[1,2-a]pyrazine-1,8-dione	0.0078	8.1079
36	4-(azetidine-1-carbonyl)-7-[5-[(2,4-difluorophenyl)methyl]-1,3-thiazol-2-yl]-9-hydroxy-4-	0.0088	8.0555

	methyl-2-propan-2-yl-3H-pyrido[1,2-a]pyrazine-1,8-dione		
37	(4R)-7-[5-[(2,4-difluorophenyl)methyl]-1,3,4-thiadiazol-2-yl]-2-ethyl-9-hydroxy-4-(methoxymethyl)-3,4-dihydropyrido[1,2-a]pyrazine-1,8-dione	0.0066	8.1805
38	(3R)-2-cyclobutyl-7-[5-[(2,4-difluorophenyl)methyl]-1,3,4-thiadiazol-2-yl]-9-hydroxy-3-(methoxymethyl)-3,4-dihydropyrido[1,2-a]pyrazine-1,8-dione	0.0075	8.1249
39	(3S)-7-[5-[(2,4-difluorophenyl)methyl]-1,3,4-thiadiazol-2-yl]-2-ethyl-9-hydroxy-3-(methoxymethyl)-3,4-dihydropyrido[1,2-a]pyrazine-1,8-dione	0.0071	8.1487
40	(3S)-2-(cyclopropylmethyl)-7-[5-[(2,4-difluorophenyl)methyl]-1,3,4-thiadiazol-2-yl]-9-hydroxy-3-(methoxymethyl)-3,4-dihydropyrido[1,2-a]pyrazine-1,8-dione	0.0073	8.1367
41	(3S)-7-[5-[(2,4-difluorophenyl)methyl]-1,3,4-thiadiazol-2-yl]-2-(2,2-dimethylpropyl)-9-hydroxy-3-(2-methoxyethoxymethyl)-3,4-dihydropyrido[1,2-a]pyrazine-1,8-dione	0.012	7.9208
42	(3S)-7-[5-[(2,4-difluorophenyl)methyl]-1,3,4-thiadiazol-2-yl]-9-hydroxy-3-(hydroxymethyl)-2-propan-2-yl-3,4-dihydropyrido[1,2-a]pyrazine-1,8-dione	0.0074	8.1308
43	N-[[(3R)-7-[5-[(2,4-difluorophenyl)methyl]-1,3,4-thiadiazol-2-yl]-9-hydroxy-1,8-dioxo-2-propan-2-yl-3,4-dihydropyrido[1,2-a]pyrazin-3-yl]methyl]acetamide	0.0086	8.0655
44	N-[[7-[5-[(2,4-difluorophenyl)methyl]-1,3-thiazol-2-yl]-9-hydroxy-4-methyl-1,8-dioxo-2-propan-2-yl-3H-pyrido[1,2-a]pyrazin-4-yl]methyl]-N-methylacetamide	0.012	7.9208
45	(4R)-7-[5-[(3,4-difluorophenyl)methyl]-1,3,4-thiadiazol-2-yl]-9-hydroxy-4-(methoxymethyl)-2-propan-2-yl-3,4-dihydropyrido[1,2-a]pyrazine-1,8-dione	0.0077	8.1135
46	(4R)-2-[(2R)-butan-2-yl]-7-[5-[(2,4-difluorophenyl)methyl]-1,3,4-thiadiazol-2-yl]-9-hydroxy-4-(methoxymethyl)-3,4-dihydropyrido[1,2-a]pyrazine-1,8-dione	0.0083	8.0809
47	(4R)-7-[5-[(2,4-difluorophenyl)methyl]-1,3,4-thiadiazol-2-yl]-9-hydroxy-4-(methoxymethyl)-2-[(2R)-3-methylbutan-2-yl]-3,4-dihydropyrido[1,2-a]pyrazine-1,8-dione	0.0098	8.0088
48	7-[5-[(2,4-difluorophenyl)methyl]-1,3-thiazol-2-yl]-9-hydroxy-N,2-dimethyl-1,8-dioxo-3,4-dihydropyrido[1,2-a]pyrazine-4-carboxamide	0.0061	8.2147
49	7-[5-[(2,4-difluorophenyl)methyl]-1,3-thiazol-2-yl]-N-ethyl-9-hydroxy-N,2,4-trimethyl-1,8-dioxo-3H-pyrido[1,2-a]pyrazine-4-carboxamide	0.0078	8.1079
50	(4S)-2-[(2R)-butan-2-yl]-7-[5-[(4-fluorophenyl)methyl]-1,3,4-thiadiazol-2-yl]-9-hydroxy-4-(methoxymethyl)-3,4-dihydropyrido[1,2-a]pyrazine-1,8-dione	0.01	8
51	(4R)-7-[5-[(2,4-difluorophenyl)methyl]-1,3,4-thiadiazol-2-yl]-9-hydroxy-4-methyl-2-propan-2-yl-4-(pyrrolidine-1-carbonyl)-3H-pyrido[1,2-a]pyrazine-1,8-dione	0.012	7.9208
52	7-[5-[(4-fluorophenyl)methyl]-1,3,4-thiadiazol-2-yl]-9-hydroxy-2-propan-2-ylspiro[4H-pyrido[1,2-a]pyrazine-3,1'-cyclopropane]-1,8-dione	0.0085	8.0706
53	(4R)-2-tert-butyl-7-[5-[(4-fluorophenyl)methyl]-1,3,4-thiadiazol-2-yl]-9-hydroxy-N,N,4-trimethyl-1,8-dioxo-3H-pyrido[1,2-a]pyrazine-4-carboxamide	0.014	7.8539
54	(4R)-2-ethyl-7-[5-[(4-fluorophenyl)methyl]-1,3,4-thiadiazol-2-yl]-9-hydroxy-N,N,4-trimethyl-1,8-dioxo-3H-pyrido[1,2-a]pyrazine-4-carboxamide	0.0084	8.0757
55	(4R)-2-ethyl-7-[5-[(4-fluorophenyl)methyl]-1,3,4-thiadiazol-2-yl]-9-hydroxy-4-methyl-4-(pyrrolidine-1-carbonyl)-3H-pyrido[1,2-a]pyrazine-1,8-dione	0.0096	8.0177
56	(4R)-N,2-diethyl-7-[5-[(4-fluorophenyl)methyl]-1,3,4-thiadiazol-2-yl]-9-hydroxy-4-methyl-1,8-dioxo-3H-pyrido[1,2-a]pyrazine-4-carboxamide	0.0095	8.0223
57	(4R)-7-[5-[(4-fluorophenyl)methyl]-1,3,4-thiadiazol-2-yl]-9-hydroxy-N-(2-methoxyethyl)-N,4-dimethyl-1,8-dioxo-2-propan-2-yl-3H-pyrido[1,2-a]pyrazine-4-carboxamide	0.013	7.8861
58	(4R)-7-[5-[(4-fluorophenyl)methyl]-1,3,4-thiadiazol-2-yl]-9-hydroxy-4-methyl-4-(morpholine-4-carbonyl)-2-propan-2-yl-3H-pyrido[1,2-a]pyrazine-1,8-dione	0.013	7.8861
59	(4R)-7-[5-[(4-fluorophenyl)methyl]-1,3,4-thiadiazol-2-yl]-9-hydroxy-4-(3-methoxyazetidine-1-carbonyl)-4-methyl-2-propan-2-yl-3H-pyrido[1,2-a]pyrazine-1,8-dione	0.012	7.9208
60	(4R)-7-[5-[(4-fluorophenyl)methyl]-1,3,4-thiadiazol-2-yl]-9-hydroxy-4-[(3R)-3-methoxypyrrolidine-1-carbonyl]-4-methyl-2-propan-2-yl-3H-pyrido[1,2-a]pyrazine-1,8-dione	0.016	7.7959
61	(4R)-7-[5-[(4-fluorophenyl)methyl]-1,3,4-thiadiazol-2-yl]-9-hydroxy-4-[(3S)-3-methoxypyrrolidine-1-carbonyl]-4-methyl-2-propan-2-yl-3H-pyrido[1,2-a]pyrazine-1,8-dione	0.014	7.8539
62	(4R)-7-[5-[(4-fluorophenyl)methyl]-1,3-thiazol-2-yl]-9-hydroxy-4-[(3R)-3-methoxypyrrolidine-1-carbonyl]-4-methyl-2-propan-2-yl-3H-pyrido[1,2-a]pyrazine-1,8-dione	0.015	7.8239
63	(4R)-7-[5-[(4-fluorophenyl)methyl]-1,3-thiazol-2-yl]-9-hydroxy-4-[(3S)-3-methoxypyrrolidine-1-carbonyl]-4-methyl-2-propan-2-yl-3H-pyrido[1,2-a]pyrazine-1,8-dione	0.016	7.7959
64	(4S)-4-(azetidine-1-carbonyl)-7-[5-[(4-fluorophenyl)methyl]-1,3-thiazol-2-yl]-9-hydroxy-4-methyl-2-propan-2-yl-3H-pyrido[1,2-a]pyrazine-1,8-dione	0.012	7.9208
65	(4S)-N-ethyl-7-[5-[(4-fluorophenyl)methyl]-1,3-thiazol-2-yl]-9-hydroxy-4-methyl-1,8-dioxo-2-propan-2-yl-3H-pyrido[1,2-a]pyrazine-4-carboxamide	0.013	7.8861

66	(4S)-7-[5-[(4-fluorophenyl)methyl]-1,3-thiazol-2-yl]-9-hydroxy-N-(2-methoxyethyl)-N,4-dimethyl-1,8-dioxo-2-propan-2-yl-3H-pyrido[1,2-a]pyrazine-4-carboxamide	0.016	7.7959
67	(4R)-7-[5-[(4-fluorophenyl)methyl]-1,3-thiazol-2-yl]-9-hydroxy-4-(3-methoxyazetidine-1-carbonyl)-4-methyl-2-propan-2-yl-3H-pyrido[1,2-a]pyrazine-1,8-dione	0.013	7.8861
68	(3S,4S)-7-[5-[(4-fluorophenyl)methyl]-1,3-thiazol-2-yl]-9-hydroxy-3-(methoxymethyl)-4-methyl-2-propan-2-yl-3,4-dihydropyrido[1,2-a]pyrazine-1,8-dione	0.01	8
69	(4S)-N,2-diethyl-7-[5-[(4-fluorophenyl)methyl]-1,3-thiazol-2-yl]-9-hydroxy-4-methyl-1,8-dioxo-3H-pyrido[1,2-a]pyrazine-4-carboxamide	0.012	7.9208
70	(4R)-7-[5-[(2-cyclopropyl-4-fluorophenyl)methyl]-1,3,4-thiadiazol-2-yl]-9-hydroxy-4-(methoxymethyl)-2-propan-2-yl-3,4-dihydropyrido[1,2-a]pyrazine-1,8-dione	0.011	7.9586
71	(3S)-2-ethyl-7-[5-[(4-fluorophenyl)methyl]-1,3-thiazol-2-yl]-9-hydroxy-N,3-dimethyl-1,8-dioxo-4H-pyrido[1,2-a]pyrazine-3-carboxamide	0.0092	8.0362
72	(3S,4S)-2-(cyclopropylmethyl)-7-[5-[(4-fluorophenyl)methyl]-1,3,4-thiadiazol-2-yl]-9-hydroxy-3-(methoxymethyl)-4-methyl-3,4-dihydropyrido[1,2-a]pyrazine-1,8-dione	0.0091	8.041
73	(3R,4R)-2-ethyl-7-[5-[(4-fluorophenyl)methyl]-1,3,4-thiadiazol-2-yl]-9-hydroxy-4-(methoxymethyl)-3-methyl-3,4-dihydropyrido[1,2-a]pyrazine-1,8-dione	0.0093	8.0315
74	(3R,4R)-2-(cyclopropylmethyl)-7-[5-[(4-fluorophenyl)methyl]-1,3,4-thiadiazol-2-yl]-9-hydroxy-4-(methoxymethyl)-3-methyl-3,4-dihydropyrido[1,2-a]pyrazine-1,8-dione	0.009	8.0458
75	(4S)-7-[5-[(4-fluorophenyl)methyl]-1,3-thiazol-2-yl]-9-hydroxy-N,N,2,4-tetramethyl-1,8-dioxo-3H-pyrido[1,2-a]pyrazine-4-carboxamide	0.0085	8.0706
76	(4S)-N-ethyl-7-[5-[(4-fluorophenyl)methyl]-1,3-thiazol-2-yl]-9-hydroxy-N,2,4-trimethyl-1,8-dioxo-3H-pyrido[1,2-a]pyrazine-4-carboxamide	0.0093	8.0315
77	(4S)-2-cyclopropyl-N-ethyl-7-[5-[(4-fluorophenyl)methyl]-1,3-thiazol-2-yl]-9-hydroxy-4-methyl-1,8-dioxo-3H-pyrido[1,2-a]pyrazine-4-carboxamide	0.011	7.9586
78	(4R)-2-ethyl-7-[5-[(4-fluorophenyl)methyl]-1,3,4-thiadiazol-2-yl]-9-hydroxy-4-(hydroxymethyl)-4-methyl-3H-pyrido[1,2-a]pyrazine-1,8-dione	0.0094	8.0269
79	(4R)-4-(azetidine-1-carbonyl)-2-[(1S)-1-cyclopropylethyl]-7-[5-[(4-fluorophenyl)methyl]-1,3-thiazol-2-yl]-9-hydroxy-4-methyl-3H-pyrido[1,2-a]pyrazine-1,8-dione	0.014	7.8539
80	(4R)-2-[(1S)-1-cyclopropylethyl]-7-[5-[(4-fluorophenyl)methyl]-1,3-thiazol-2-yl]-9-hydroxy-N,N,4-trimethyl-1,8-dioxo-3H-pyrido[1,2-a]pyrazine-4-carboxamide	0.014	7.8539
81	(4R)-2-[(1S)-1-cyclopropylethyl]-N-ethyl-7-[5-[(4-fluorophenyl)methyl]-1,3-thiazol-2-yl]-9-hydroxy-4-methyl-1,8-dioxo-3H-pyrido[1,2-a]pyrazine-4-carboxamide	0.016	7.7959
82	(4R)-2-[(1R)-1-cyclopropylethyl]-7-[5-[(4-fluorophenyl)methyl]-1,3-thiazol-2-yl]-9-hydroxy-4-(3-methoxyazetidine-1-carbonyl)-4-methyl-3H-pyrido[1,2-a]pyrazine-1,8-dione	0.016	7.7959
83	(4R)-2-[(1R)-1-cyclopropylethyl]-N-ethyl-7-[5-[(4-fluorophenyl)methyl]-1,3-thiazol-2-yl]-9-hydroxy-4-methyl-1,8-dioxo-3H-pyrido[1,2-a]pyrazine-4-carboxamide	0.018	7.7447
84	(3R)-2-ethyl-7-[5-[(4-fluorophenyl)methyl]-1,3,4-thiadiazol-2-yl]-9-hydroxy-3-propan-2-yl-3,4-dihydropyrido[1,2-a]pyrazine-1,8-dione	0.0078	8.1079
85	(3S)-2-ethyl-7-[5-[(4-fluorophenyl)methyl]-1,3,4-thiadiazol-2-yl]-9-hydroxy-3-propan-2-yl-3,4-dihydropyrido[1,2-a]pyrazine-1,8-dione	0.008	8.0969
86	(3R,4S)-7-[5-[(4-fluorophenyl)methyl]-1,3,4-thiadiazol-2-yl]-9-hydroxy-4-(methoxymethyl)-3-methyl-2-propan-2-yl-3,4-dihydropyrido[1,2-a]pyrazine-1,8-dione	0.0088	8.0555
87	(3R)-2-ethyl-7-[5-[(4-fluorophenyl)methyl]-1,3-thiazol-2-yl]-9-hydroxy-N,N,3-trimethyl-1,8-dioxo-4H-pyrido[1,2-a]pyrazine-3-carboxamide	0.0096	8.0177
88	(3R)-2-ethyl-7-[5-[(4-fluorophenyl)methyl]-1,3-thiazol-2-yl]-9-hydroxy-3-methyl-3-(pyrrolidine-1-carbonyl)-4H-pyrido[1,2-a]pyrazine-1,8-dione	0.011	7.9586
89	(3S)-7-[5-[(4-fluorophenyl)methyl]-1,3,4-thiadiazol-2-yl]-9-hydroxy-3-(methoxymethyl)-2-pentan-3-yl-3,4-dihydropyrido[1,2-a]pyrazine-1,8-dione	0.012	7.9208
90	(3R,4S)-2-ethyl-7-[5-[(4-fluorophenyl)methyl]-1,3,4-thiadiazol-2-yl]-9-hydroxy-3-(methoxymethyl)-4-methyl-3,4-dihydropyrido[1,2-a]pyrazine-1,8-dione	0.009	8.0458
91	(3R,4S)-7-[5-[(4-fluorophenyl)methyl]-1,3,4-thiadiazol-2-yl]-9-hydroxy-3-(methoxymethyl)-4-methyl-2-propan-2-yl-3,4-dihydropyrido[1,2-a]pyrazine-1,8-dione	0.0098	8.0088
92	(4R)-2-[(1R)-1-cyclopropylethyl]-7-[5-[(4-fluorophenyl)methyl]-1,3,4-thiadiazol-2-yl]-9-hydroxy-4-(methoxymethyl)-3,4-dihydropyrido[1,2-a]pyrazine-1,8-dione	0.0099	8.0044
93	(3S,4R)-7-[5-[(4-fluorophenyl)methyl]-1,3,4-thiadiazol-2-yl]-9-hydroxy-3-(methoxymethyl)-4-methyl-2-propan-2-yl-3,4-dihydropyrido[1,2-a]pyrazine-1,8-dione	0.0091	8.041
94	(3S)-3-(azetidine-1-carbonyl)-7-[5-[(4-fluorophenyl)methyl]-1,3,4-thiadiazol-2-yl]-9-hydroxy-3-methyl-2-propan-2-yl-4H-pyrido[1,2-a]pyrazine-1,8-dione	0.0099	8.0044
95	(4R)-7-[5-[(4-fluorophenyl)methyl]-1,3,4-thiadiazol-2-yl]-9-hydroxy-N,N,2,4-tetramethyl-	0.0097	8.0132

	1,8-dioxo-3H-pyrido[1,2-a]pyrazine-4-carboxamide		
96	(4R)-7-[5-[(4-fluorophenyl)methyl]-1,3-thiazol-2-yl]-9-hydroxy-N,N,2,4-tetramethyl-1,8-dioxo-3H-pyrido[1,2-a]pyrazine-4-carboxamide	0.0079	8.1024
97	(3R)-2-ethyl-7-[5-[(4-fluorophenyl)methyl]-1,3,4-thiadiazol-2-yl]-9-hydroxy-3-methyl-3,4-dihydropyrido[1,2-a]pyrazine-1,8-dione	0.0071	8.1487
98	(3S)-7-[5-[(4-fluorophenyl)methyl]-1,3,4-thiadiazol-2-yl]-9-hydroxy-3-[(1S)-1-methoxyethyl]-2-propan-2-yl-3,4-dihydropyrido[1,2-a]pyrazine-1,8-dione	0.0091	8.041
99	(4R)-7-[5-[(2,4-difluorophenyl)methyl]-1,3-thiazol-2-yl]-9-hydroxy-N,N,2,4-tetramethyl-1,8-dioxo-3H-pyrido[1,2-a]pyrazine-4-carboxamide	0.0072	8.1427
100	(3S)-7-[5-[(4-fluorophenyl)methyl]-1,3,4-thiadiazol-2-yl]-9-hydroxy-3-(hydroxymethyl)-2-propan-2-yl-3,4-dihydropyrido[1,2-a]pyrazine-1,8-dione	0.008	8.0969
101	(3S,4S)-7-[5-[(4-fluorophenyl)methyl]-1,3,4-thiadiazol-2-yl]-9-hydroxy-4-(methoxymethyl)-3-methyl-2-propan-2-yl-3,4-dihydropyrido[1,2-a]pyrazine-1,8-dione	0.0089	8.0506
102	(4R)-7-[5-[(4-fluorophenyl)methyl]-1,3,4-thiadiazol-2-yl]-9-hydroxy-2-propan-2-yl-4-(propan-2-yloxymethyl)-3,4-dihydropyrido[1,2-a]pyrazine-1,8-dione	0.012	7.9208
103	(4S)-7-[5-[(4-fluorophenyl)methyl]-1,3-thiazol-2-yl]-9-hydroxy-4-[(1R)-1-methoxyethyl]-2-propan-2-yl-3,4-dihydropyrido[1,2-a]pyrazine-1,8-dione	0.011	7.9586
104	(4R)-4-[(1R)-1-ethoxypropyl]-7-[5-[(4-fluorophenyl)methyl]-1,3,4-thiadiazol-2-yl]-9-hydroxy-2-propan-2-yl-3,4-dihydropyrido[1,2-a]pyrazine-1,8-dione	0.014	7.8539
105	(4R)-N-ethyl-7-[5-[(4-fluorophenyl)methyl]-1,3-thiazol-2-yl]-9-hydroxy-4-(methoxymethyl)-1,8-dioxo-2-propan-2-yl-3H-pyrido[1,2-a]pyrazine-4-carboxamide	0.015	7.8239
106	(4R)-N-ethyl-7-[5-[(4-fluorophenyl)methyl]-1,3,4-thiadiazol-2-yl]-9-hydroxy-4-(methoxymethyl)-N-methyl-1,8-dioxo-2-propan-2-yl-3H-pyrido[1,2-a]pyrazine-4-carboxamide	0.015	7.8239
107	(4R)-N-ethyl-7-[5-[(4-fluorophenyl)methyl]-1,3,4-thiadiazol-2-yl]-9-hydroxy-4-(2-methoxyethoxymethyl)-N-methyl-1,8-dioxo-2-propan-2-yl-3H-pyrido[1,2-a]pyrazine-4-carboxamide	0.019	7.7212

Data Preprocessing

The downloaded CSV file was opened in Microsoft Excel, where the dataset was systematically cleaned and organized to retain only the retain only the relevant columns containing SMILES and IC50 values for further analysis. To transform the IC_{50} values (reported in μM) into their corresponding pIC_{50} values, the following formula was used: **[PIC50 = 6 – Log (IC50)]**

Descriptor Generation

The curated dataset, including chemical structures and pIC_{50} values, was then imported into **Chemmaster 1.2 – Basic**, a free molecular modeling tool available on the Crescent Silico website (https://crescent-silico.com/chemmaster). For each molecule, SMILES strings were entered using the "Structure from SMILES" option under the "Structure" tab to generate 2D chemical structures. Following structure generation, the pIC_{50} column was imported into the software via the "File > Import Columns" feature, and the working file was saved in the (*.proj) format for continuity. Subsequently, the data column containing pIC_{50} values was again exported in CSV format**.** Under the "Calculate" tab, the software computed a range of molecular descriptors, including: Molecular Weight, LogP, Molar Refractivity, Hydrogen Bond Acceptors (HBA), Hydrogen Bond Donors (HBD), Number of Rotatable Bonds, Quantitative Estimate of Drug-Likeness (QED). These descriptors numerically represent the physicochemical properties of the molecules and are essential variables in establishing structure-activity relationships.

QSAR Model Development

To initiate QSAR modeling, the QSAR tab was accessed, and the "Build Model" option was selected. All computed molecular descriptors were assigned as independent variables (X), while the pIC_{50} values served as the dependent variable (Y) representing biological activity. The dataset was divided into training and test sets using the software's Dataset Division tool, with 75% of the compounds allocated for model training and 25% for testing. This ensured that the model could be evaluated on unseen data for its predictive ability.

Model Validation

Model development was performed using the Multiple Linear Regression (MLR) method under the "Model Settings" tab. To internally validate the robustness of the model, the Q^2 (cross-validation, leave-one-out or CV-LOO) method was selected and computed**.** The final model's performance was assessed using statistical parameters such as: **R^2** (coefficient of determination), **RMSE** (Root Mean Square Error), **MAE** (Mean Absolute Error)**, Q^2 (CV-LOO)** (cross-validated coefficient).

HQSAR Analysis

Data Collection

The previously curated dataset, consisting of substituted thiazole derivatives along with their pIC_{50} values, was utilized for HQSAR modeling. The cleaned and processed dataset was imported into Chemmaster 1.2 – Basic by opening the previously saved project file. The saved columns containing the molecular structures (in

SMILES format) and corresponding pIC_{50} values were reloaded into the workspace for further analysis.

Molecular Fingerprint Generation

To enable HQSAR modeling, molecular fingerprints were generated using the Morgan fingerprint algorithm, which is known for its ability to capture substructural features and molecular topology. These fingerprints were selected as the fixed X-variables for establishing the structure–activity relationship. The Morgan fingerprints serve as encoded numerical representations of molecular structure and were essential in building a predictive HQSAR model.

HQSAR Model Building

To initiate the HQSAR model development, the "QSAR" tab was accessed within Chemmaster, and the Build HQSAR model option was selected. The biological activity data (pIC_{50} values) were set as the dependent variable (Y-variable), while the Morgan fingerprints were assigned as the independent variables (X-variables). This setup was used to correlate the molecular structural features with their corresponding inhibitory activity.

Model Validation

The dataset was divided into two subsets using a predefined ratio, with 75% of the compounds used for training the model and 25% reserved for testing its predictive performance. After confirming all model settings, the model generation was initiated by clicking the "OK" button. The resulting HQSAR model was then evaluated using standard validation metrics, including **R^2** for training and test set, to ensure reliability and robustness, **RMSE**, Lower values indicate better predictive accuracy; typically close to 0. Like RMSE, lower MAE values indicate better model performance. Good MAE values depend on dataset scale but should ideally be **<0.5** for pIC_{50} models.

RESULT AND DISCUSSIONS

QSAR Model

The QSAR model was successfully built using Multiple Linear Regression (MLR) with 9 molecular descriptors. The model showed excellent predictive performance for both the training and test sets. The scatter plot (Fig visualizes the relationship between the predicted and actual values of the target property (PIC50). In the X-Axis, Predicted values from the QSAR model. In Y-Axis, Actual PIC50 values. Red Dots indicates Training set molecules. Blue Dots indicates Test set molecules. The orange line represents the ideal y = x relationship, where predicted values perfectly match actual values.

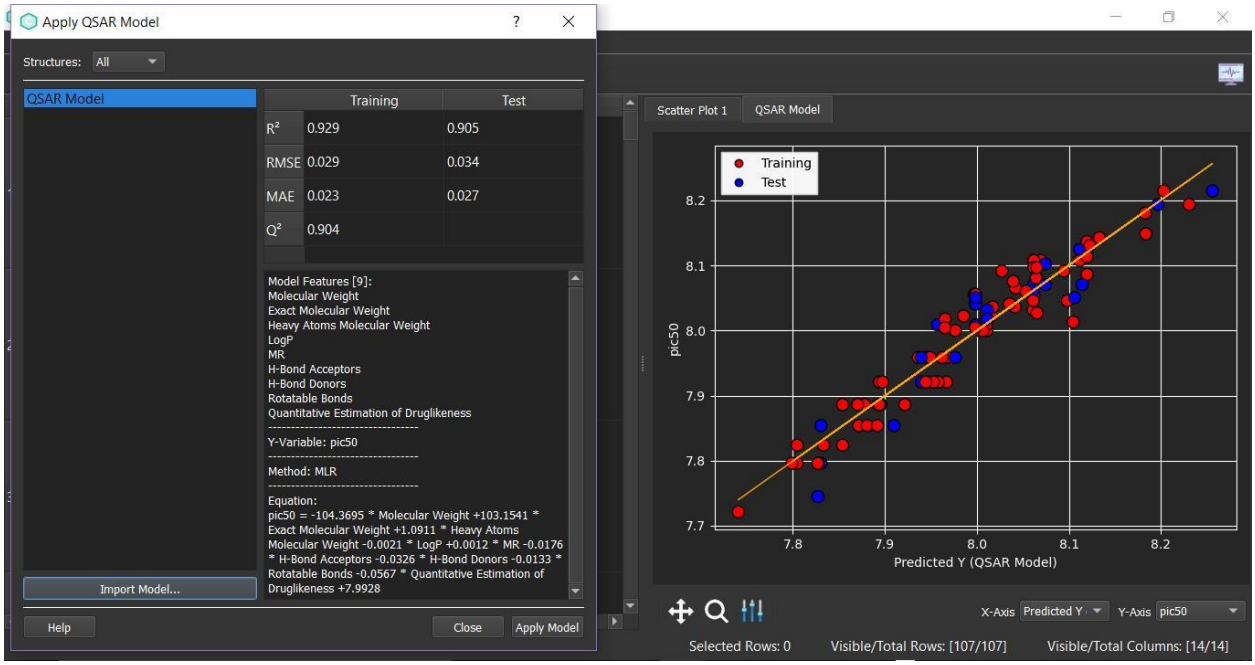

Figure 5: Predicted vs. Actual pIC_{50} values using MLR- based QSAR model with training and test set distribution.

Table 2: Performance Metrics of QSAR Model.

Metric	Training Set	Test Set	Range
R^2 (Coefficient of Determination)	0.929	0.905	excellent correlation and model fit.
RMSE (Root Mean Square Error)	0.029	0.034	Minimizes the model's prediction error.
MAE (Mean Absolute Error)	0.023	0.027	simple indicator of prediction accuracy
Q2(Cross Validated R^2)	0.904	-	robust and reliable model

HQSAR Model

In X-axis**,** Predicted values from the HQSAR model. In Y-axis, Experimental (actual) values. **Red dots:** Training set molecules (used to build the model). **Blue dots:** Test set molecules (used to evaluate predictive performance.

Clustering Near the Line: Both training and test are close to the orange line, indicating that the HQSAR model's predictions are in strong agreement with the experimental data. This visual agreement is a key indicator of model reliability and predictive power.

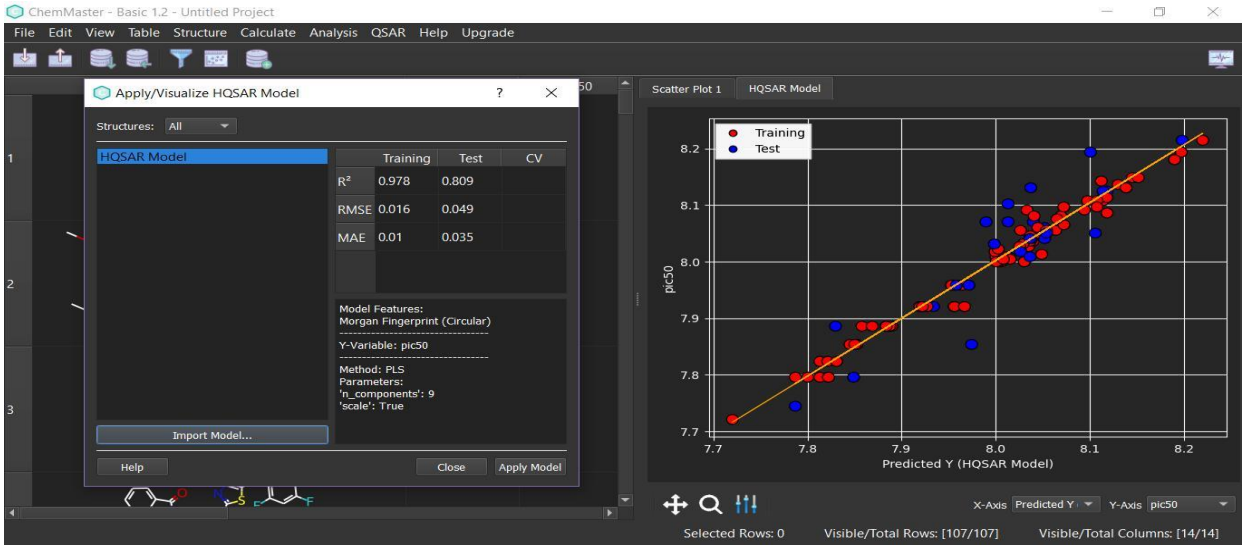

Figure 6: Predicted vs. Actual pIC_{50} values using HQSAR model with training and test set distribution.

Table 3: Performance Metrics of HQSAR Model.

Metric	Training Set	Test Set	Range
R2	0.951	0.812	better fit; good model.
RMSE	0.024	0.049	Lower values indicate better predictive accuracy
MAE	0.018	0.038	lower MAE values indicate better model performance

Following the development of the HQSAR model, the structure–activity relationship was further interpreted using fragment contribution analysis. Upon selecting the "Visualize HQSAR Model" option under the QSAR tab, the Chemical Structures Panel displayed multiple molecular representations in SMILES format. Each molecule was decomposed into fragments, and their respective contributions to biological activity were quantified. The "Fragment" column listed the specific structural moieties, alongside the number of atoms involved and their associated coefficients. Fragments with positive coefficients were visualized as red-highlighted atoms (Fig:7), indicating a favorable contribution to the biological activity (increase in pIC_{50}), while negative coefficients were shown as blue-highlighted atoms (Fig:8), reflecting a detrimental effect.

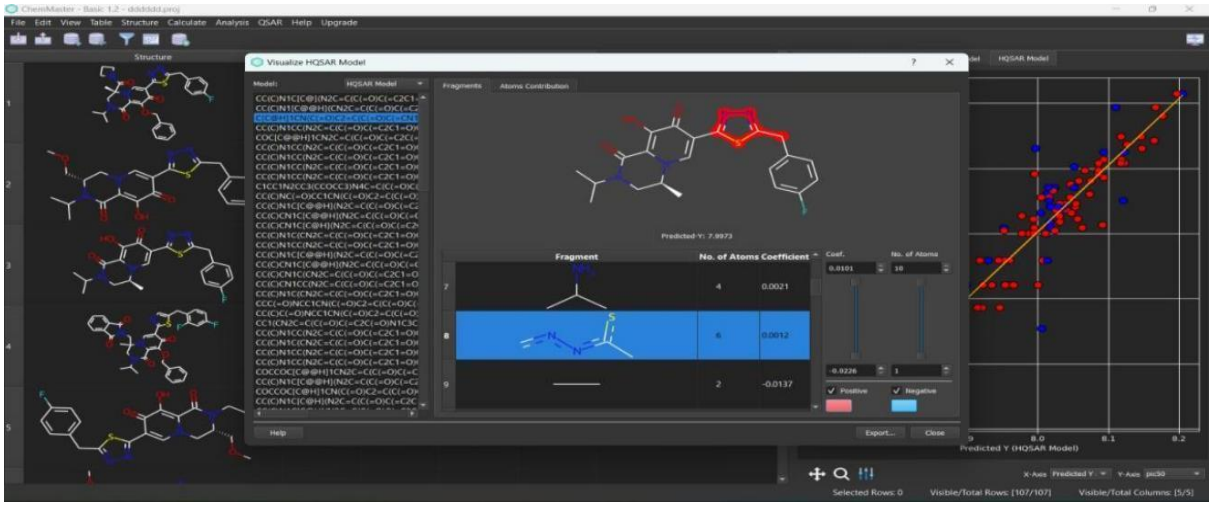

Figure 7: The red ring in the compound structure (a substituted thiazole ring) indicates a positively contributing fragment that influence biological activity (increase pIC50).

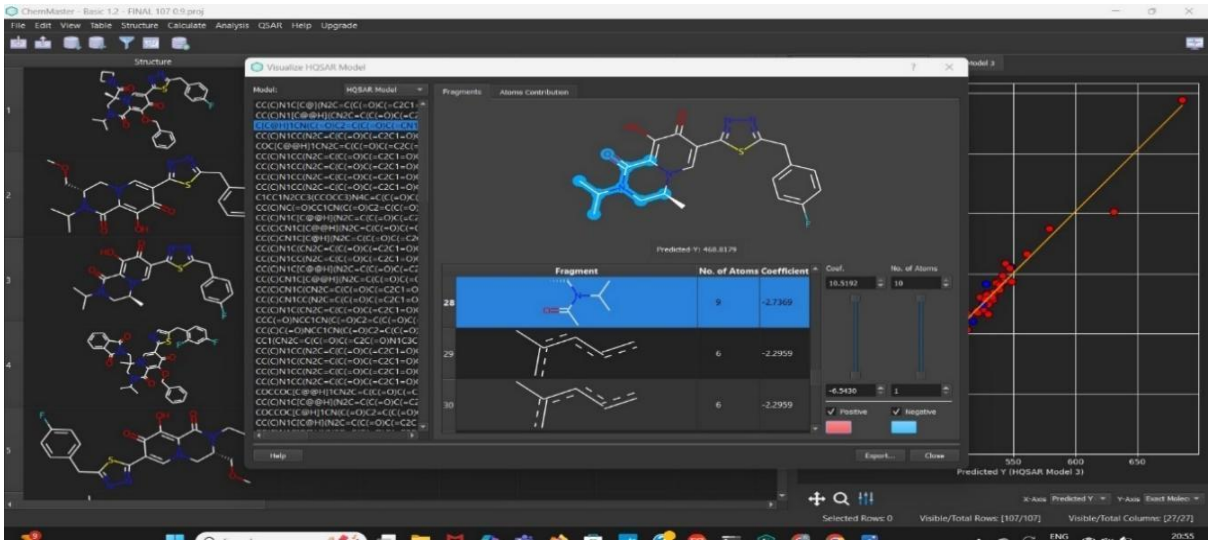

Figure 8: This ring is shown in blue because it negatively affects the activity of the molecule. This means that when this ring is present in the molecule, the predicted biological activity decreases. Therefore, Removing or modifying this ring could potentially improve the activity of the compound.

The HQSAR model also enables intuitive visualization of fragment contributions through a color-coded 2D structural map, aiding in the interpretation of structure–activity relationships.

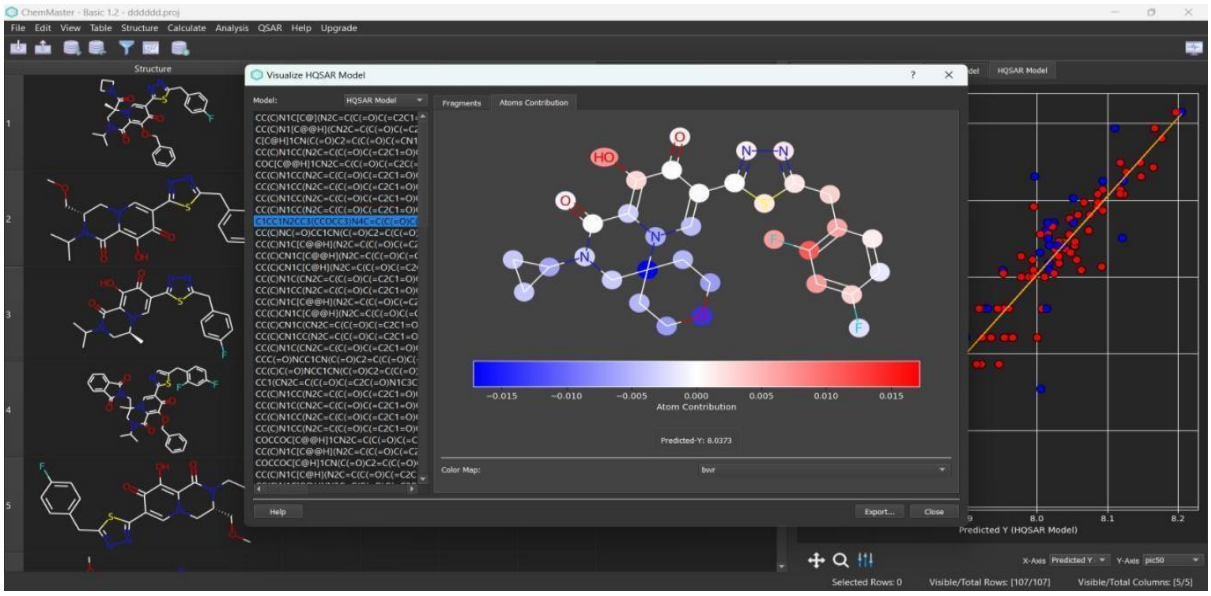

Figure 9: HQSAR color-coded 2D structure showing atomic contributions to predicted pIC_{50} using bwr gradient scale.

In the middle panel, the 2D chemical structure of a selected compound is displayed with atoms highlighted based on their contribution to the predicted biological activity. The visualization employs the bwr (blue-white-red) color gradient scale (Fig:9), where each color corresponds to the strength and nature of the fragment's influence on activity. According to the color map, dark blue (≤ -0.015) indicates a strong negative contribution, while light blue (~ -0.005) represents a mild negative contribution. White (0.000) signifies a neutral or negligible effect, light red (~ +0.005) denotes a mild positive contribution, and dark red (≥ +0.015) reflects a strong positive contribution to biological activity.

For the selected compound, the HQSAR model predicted a pIC_{50} value of 8.0373, indicating high inhibitory potency. The atom-level color distribution clearly illustrates the key structural features that either enhance or reduce the compound's activity, thus guiding rational design for further structural optimization.

CONCLUSION

This study developed a robust QSAR model to predict antiviral activity against HIV-1 integrase using a curated dataset of compounds with known Anti-HIV activity. Molecular descriptors were computed and refined via ChemMaster 1.2, and key features were selected. The model demonstrated strong predictive performance,

validated through cross-validation, and test sets, ensuring its reliability. Visualization of HQSAR model highlighted the thiazole ring as a key contributor to antiviral activity, suggesting its importance as a favorable heterocyclic ring. Overall, this computational approach provides valuable guidance for understanding the relationship between molecular descriptors and biological activity.

FUTURE SCOPE WORK

The present study successfully developed QSAR and HQSAR models for substituted thiazoles as HIV integrase inhibitors, demonstrating strong predictive performance. In the future, this work can be extended by incorporating a more diverse chemical dataset to enhance model robustness and reliability. Additionally, targeting other key HIV enzymes such as reverse transcriptase and protease may enable multi-target drug design. Integrating advanced machine learning technique- deep learning could further improve prediction and accuracy. Moreover, experimental validation of the top-ranked compounds would be essential to confirm their biological activity and therapeutic potential.

REFERENCES

1. Crisan L, Bora A. Small molecules of natural origin as potential anti-HIV agents: a computational approach. Life, 2021 Jul 20; 11(7): 722.
2. Abd Elkodous M, El-Sayyad GS, Nasser HA, Elshamy AA, Morsi M, AbdelrahmanIY, Kodous AS, Mosallam FM, Gobara M, El-Batal AI. Engineered nanomaterials as potential candidates for HIV treatment: between opportunities and challenges. Journal of Cluster Science, 2019 May 15; 30(3): 531-40. DOI: 10.1007/s10876-019-01533-8.
3. Tripathi KD. Essentials of medical pharmacology. Jaypee Brothers medical publishers, 2018 Oct 31.
4. Deeks SG, Overbaugh J, Phillips A, Buchbinder S. HIV infection (Primer). Nature Reviews: Disease Primers, 2015; 1(1).
5. Liao C, Nicklaus MC. Computer tools in the discovery of HIV-1 integrase inhibitors. Future medicinal chemistry, 2010 Jul 1; 2(7): 1123-40.
6. Katlama C, Murphy R. Emerging role of integrase inhibitors in the management of treatment-experienced patients with HIV infection. Therapeutics and Clinical Risk Management, 2009 May 4: 331-40.
7. Mahajan PS, Smith SJ, Li M, Craigie R, Hughes SH, Zhao XZ, Burke Jr TR. N- Substituted Bicyclic Carbamoyl Pyridones: Integrase Strand Transfer Inhibitors that Potently Inhibit Drug-Resistant HIV-1 Integrase Mutants. ACS Infectious Diseases, 2024 Feb 12; 10(3): 917-27.
8. Peter SC, Dhanjal JK, Malik V, Radhakrishnan N, Jayakanthan M, Sundar D. Quantitative structure-activity relationship (QSAR): modeling approaches to biological applications. Encyclopedia of bioinformatics and computational biology, 2019: 661-76.
9. Verma J, Khedkar VM, Coutinho EC. 3D-QSAR in drug design-a review. Current topics in medicinal chemistry, 2010 Jan 1; 10(1): 95-115.
10. Bouamrane S, Khaldan A, Alaqarbeh M, Sbai A, Ajana MA, Lakhlifi T, Bouachrine M, Maghat H. Computational integration for antifungal 1, 2, 4-triazole inhibitors design: QSAR, molecular docking, molecular dynamics simulations, ADME/Tox, and retrosynthesis studies. Chemical Physics Impact, 2024 Jun 1; 8: 100502.
11. Palangsuntikul R, Berner H, Berger ML, Wolschann P. Holographic quantitative structure-activity relationships of tryptamine derivatives at NMDA, 5HT1A and 5HT2A receptors. Molecules, 2013 Jul 24; 18(8): 8799-811.
12. Li Q, Cheng T, Wang Y, Bryant SH. PubChem as a public resource for drug discovery. Drug discovery today, 2010 Dec 1; 15(23-24): 1052-7.
13. Cheng T, Pan Y, Hao M, Wang Y, Bryant SH. PubChem applications in drug discovery: a bibliometric analysis. Drug discovery today, 2014 Nov 1; 19(11): 1751-6.
14. ChemMaster. CrescentSilico. 2023 https: //crescentsilico.wordpress.com/chemmaster/
15. National Center for Biotechnology Information. "PubChem Bioassay Record for AID 1795460, Source: BindingDB"*PubChem*, https: //pubchem.ncbi.nlm.nih.gov/bioassay/1795460